Available online at www.sciencedirect.com
SCIENCE DIRECT®
Plasmid 50 (2003) 120–130
PLASMID
www.elsevier.com/locate/yplas

Non-cytotoxic variants of the Kid protein that retain their auto-regulatory activity

Sandra Santos-Sierra,[a,1,2] Marc Lemonnier,[a,2] Belen Nuñez,[a] David Hargreaves,[b] John Rafferty,[b] Rafael Giraldo,[a] Jose Manuel Andreu,[a] and Ramon Díaz-Orejas[a,*]

[a] *Departemento de Microbiologia Molecular, Centro de Investigaciones Biológicas, CSIC, Velázquez 144, Madrid E-28006, Spain*
[b] *Department of Molecular Biology and Biotechnology, Krebs Institute for Biomolecular Research, University of Sheffield, Sheffield S10 2TN, UK*

Received 30 April 2003, revised 19 May 2003

Abstract

Kid and Kis are, respectively, the toxin and antitoxin encoded by the *parD* operon of plasmid R1. The recently solved crystal structure of Kid has revealed that this protein closely resembles the CcdB toxin of plasmid F. In CcdB, the residues involved in toxicity are located at the carboxy-terminal end of the protein. However, an analogous information on the Kid toxin was not available. Here, we have characterized a collection of non-toxic mutants of the Kid protein and identified the residues that affected the toxicity but not the co-regulatory activity of Kid. These are located in two discrete regions of the protein, at the amino and carboxy-terminal ends. Particularly, residues E18 and R85, that are conserved in the *Escherichia coli* ChpAK and RelE toxins, are affected by amino-acid changes that alter neither the overall structure of the protein nor its state of association, as shown by CD and sedimentation equilibrium analyses. However, thermal denaturation and intrinsic tryptophan fluorescence emission data point to subtle local changes at the N-terminal end of the protein. The implications of these results in the current model on the structure and function of Kid-related bacterial toxins are discussed.
© 2003 Elsevier Science (USA). All rights reserved.

Keywords: Kid; *parD*; Toxin–antitoxin systems; CD; Fluorescence; Protein structure

1. Introduction

Toxin–antitoxin modules (TA) are found in several plasmids as well as in bacterial and archaeal chromosomes (Gerdes, 2000). In general, these modules are bicistronic operons in which the antitoxin gene is located upstream of the toxin gene. The TA-encoded toxins interact with their antitoxin partners to form a non-toxic complex that auto-regulates the expression of the TA operon. Under certain conditions, however, the toxins target particular host functions to inhibit cell proliferation (Gerdes, 2000). In some cases, the mode of action of the toxins has been substantially

* Corresponding author. Fax: +34-91-562-7518.
E-mail address: ramondiaz@cib.csic.es (R. Díaz-Orejas).
[1] Present mailing address: Institut für Biochemische Pharmakologie, Universität Innsbruck, Peter Mayr Strasse 1, A-6020 Innsbruck, Austria.
[2] These authors contributed equally to this work.

0147-619X/$ - see front matter © 2003 Elsevier Science (USA). All rights reserved.
doi:10.1016/S0147-619X(03)00048-9

clarified: the F-plasmid-encoded CcdB toxin targets the GyrA subunit of the *Escherichia coli* topoisomerase II, DNA gyrase (Bernard and Couturier, 1992), while the *E. coli* RelE toxin inhibits protein synthesis by cleaving mRNA in the ribosomal A site (Pedersen et al., 2003). In other cases, the targets of the toxins have not been identified, albeit inhibition of particular cellular functions has been observed: for example, the ChpAK toxin inhibits protein synthesis and DNA replication (Pedersen et al., 2002), and the Kid toxin of plasmid R1 inhibits plasmid ColE1 replication in vivo and in vitro (Potrykus et al., 2002; Ruiz-Echevarría et al., 1995). In addition, an emerging focus on the structural biology of TA modules has led to the resolution of the three dimensional structures of two toxins: CcdB (Loris et al., 1999), and more recently, Kid (Hargreaves et al., 2002b). Kid–Kis and CcdB–CcdA form the toxin–antitoxin pairs respectively encoded by the TA modules *parD* of plasmid R1 (Bravo et al., 1987; Ruiz-Echevarría et al., 1995) and *ccd* of plasmid F (Ogura and Hiraga, 1983). Remarkably, the crystal structure of Kid has revealed that this toxin is a dimer with twofold symmetry that closely resembles CcdB, despite a low similarity in their amino-acid sequences (Hargreaves et al., 2002b). Moreover, *parD* and *ccd* have the archetypal genetic organization of TA modules and, in both cases, a tight regulatory interaction of the toxin with its antitoxin (Ruiz-Echevarría et al., 1991a; Tam and Kline, 1989; Tsuchimoto and Ohtsubo, 1993). However, the mode of action of both toxins must be different, since the CcdB toxin triggers the SOS response in *E.coli*, while Kid does not (Ruiz-Echevarría et al., 1991b).

A mutational analysis on CcdB led to the identification of a region in the protein that is potentially involved in the specific interaction with its target. The mutations that disrupt the toxicity of the protein without affecting its coregulation activity were found to affect the last three C-terminal residues of the toxin (Bahassi et al., 1995). The same analysis made on the Kid toxin, that could tell us whether these two structurally similar toxins conserve the same interface of interaction with their targets, was not available to date. In the present work, we address this issue by performing a detailed analysis of non-toxic variants of the Kid protein that were isolated in a former genetic approach (Hargreaves et al., 2002b).

2. Materials and methods

2.1. Bacterial strains

Bacteria used in this study were *E. coli* K12 strains: OV2 (F$^-$, *leu*, *thyA* (*deo*), *ara* (*am*), *lac*$^-$ 125 (*am*), *galU42*, *galE*, *trp* (*am*), *tsx* (*am*), *tyrT* (*supF*(*ts*)*A81*), *ile*, *his*), as host for plasmid pAB1120; C600 (*leuB6*, *thr-1*, *thi-1*, *supE44*, *lacY1*, *rfbD1*, *fhuA21*, r^+m^+), for protein overproduction; and MLM373 (*Δ(lac, pro)*, *supE*, *thi*), that was obtained as a spontaneous F$^-$ derivative of CSH16 (Miller, 1972), and was used for β-galactosidase assays.

2.2. Construction of plasmids

Plasmids used and constructed in this work are listed in Table 1.

To construct the derivatives of pRG-recA-Nhis (Table 1), PCR fragments encoding *kis74* and *kid* wild-type or mutant alleles were generated using primers *PKIDB(+)* (5′CGGGGATCCGTCAG GAGGAAATCTGAC; *Bam*HI site underlined), and *PKIS80(-)* (5′CTTTTACCGCGGGGCAG CATGCATACCACC) which introduces a *Sac*II site (underlined) plus a sequence coding for the thrombin cleavage site at 5′ of *kis*. The resulting fragments were inserted into the pRG-recA-Nhis vector digested with *Sac*II and *Bam*HI yielding pRG-his-1120 plasmid and its mutant counterparts.

The pMLM132 plasmid resulted from the trimolecular ligation of: (i) a 604-bp fragment containing the *parD* operator/promoter sequences obtained from PCR amplification using primers *parD51* (5′CTGATGTACCTGCTGTGT) and *parD3Bam* (5′GGCCGGATCCATTCT TCACCT CCATAAA) and subsequent digestion with *Pvu*II and *Bam*HI; (ii) a 3260-bp fragment containing *lacZ* resulting from digestion of pRS551 (Simons et al., 1987) with *Bam*HI and *Dra*I; (iii) a 7505-bp

Table 1
Plasmids used and constructed in this study

Plasmid	Relevant characteristics[a]	Reference/source
pAB1120	R1, *copB*$^-$, *parD* (*kis74*, *kid[wt]*), *kan*	Bravo et al. (1988)
pAB1120-V9I	pAB1120 (*kis74*, *kid[V9I]*)	Hargreaves et al. (2002b)
pAB1120-E18K	pAB1120 (*kis74*, *kid[E18K]*)	Hargreaves et al. (2002b)
pAB1120-G21R	pAB1120 (*kis74*, *kid[G21R]*)	Hargreaves et al. (2002b)
pAB1120-V25M	pAB1120 (*kis74*, *kid[V25M]*)	Hargreaves et al. (2002b)
pAB1120-T29I	pAB1120 (*kis74*, *kid[T29I]*)	Hargreaves et al. (2002b)
pAB1120-G70S	pAB1120 (*kis74*, *kid[G70S]*)	Hargreaves et al. (2002b)
pAB1120-R73H	pAB1120 (*kis74*, *kid[R73H]*)	Hargreaves et al. (2002b)
pAB1120-D75N	pAB1120 (*kis74*, *kid[D75N]*)	Hargreaves et al. (2002b)
pAB1120-D81N	pAB1120 (*kis74*, *kid[D81N]*)	Hargreaves et al. (2002b)
pAB1120-R85W	pAB1120 (*kis74*, *kid[R85W]*)	Hargreaves et al. (2002b)
pAB1120-P94L	pAB1120 (*kis74*, *kid[P94L]*)	Hargreaves et al. (2002b)
pRG-recA-NHis	pUC18, *recA* promoter (p*recA*), Φ_{10} leader sequence, his_6, cutting site for thrombine, *bla*	Giraldo et al. (1998)
pRG-his-1120	pRG-recA-Nhis, p*recA*::his_6::*kis74*, *kid[wt]*	This work
pKisKidE18K	pRG-recA-Nhis, p*recA*::his_6::*kis74*, *kid[E18K]*	This work
pKisKidR85W	pRG-recA-Nhis, p*recA*:: his_6::*kis74*, *kid[R85W]*	This work
pMLM1	mini-F, *repFIA*$^+$, *sop*$^+$, *cat*	Lemonnier et al. (2000)
pMLM132	pMLM1, p*parD*::*lacZ*,	This work
pRS551	pMB1, *lacZYA*$^+$, *bla*, *kan*	Simons et al. (1987)

[a] *bla*, *cat*, and *kan* denote genes conferring resistance to ampicillin, chloramphenicol, and kanamycin, respectively.

fragment containing the mini-F sequences for replication and partition, and the *cat* gene, obtained from digestion of the pMLM1 plasmid (Lemonnier et al., 2000) with *Bam*HI and subsequent end-filling with Klenow.

2.3. Protein purification

The purification of Kid and its different mutants was performed with a protocol identical to that described for the wild-type protein by Hargreaves et al. (2002a). Briefly, lysates were prepared from induced cultures of *E. coli* C600 strains overproducing Kid mutants together with the His_6-tagged Kis protein (from pRG-recA-Nhis derivatives; Table 1). Lysates were clarified and the soluble fraction was loaded onto a Ni^{2+}-affinity column. The complexes between each of the Kid mutants and His_6-Kis remained tightly bound to the affinity column. To release the strong interaction between the Kis antidote and the Kid mutants, it was required to denature Kid using guanidine–HCl. Refolding of the protein was accomplished by a dialysis procedure (Giraldo et al., 1998). Finally, the sample was loaded onto a SP-Sepharose column and the bound Kid was eluted using a KCl gradient.

2.4. Analytical ultracentrifugation

The association state of Kid wild-type and mutant proteins was studied by means of sedimentation equilibrium. The experiments were performed in an XL-A analytical ultracentrifuge (Beckman Coulter, Fullerton, CA) equipped with UV–VIS absorbance optics, using six-channel centerpieces of 12-mm path length. The different proteins (70 μl), ranging in protein concentration from 5 to 45 μM in potassium phosphate 100 mM, pH 7.0, were sedimented at a speed of 15, 19, and 25 Krpm at 20 °C. When sedimentation equilibrium was reached, the radial absorbance in each compartment was scanned at three different wavelengths (230, 255, and 280 nm) depending on the concentration of protein used. High speed sedimentation (48 Krpm) was conducted afterwards for baseline correction in all the cases. The buoyant molecular masses of the proteins were determined by fitting a sedimentation equilibrium model for a single sedimenting

solute to individual datasets with the EQASSOC program (supplied by Beckman; see Minton, 1994). The partial specific volume of Kid was 0.742 ml/g. Sedimentation velocity experiments were performed with double sector cells in 50 mM Tris, 100 mM KCl, pH 8.0, at 20 °C with Kid concentrations ranging between 33 and 150 μM. They were analyzed using XLAVEL and VELGAMMA (supplied by Beckman).

2.5. Circular dichroism spectroscopy

CD measurements in the far UV were obtained with a Jasco J-720 spectropolarimeter using 0.1-cm path length quartz cuvettes in a thermostated cell holder at 5 °C. The protein concentration used was 15 μM, in potassium phosphate buffer 100 mM, pH 7.0. Ten spectra were averaged for each sample with the following parameters: step resolution 0.2 nm, speed 50 nm/min, response 1 s, bandwidth 1.0 nm. The spectrum of the buffer was substrated as blank. The raw ellipticity data (millidegrees) were transformed to mean molar ellipticity per residue $[\Theta]_{MRW\,222}$ (deg cm^2/dmol). The content of secondary structure was estimated from the far UV CD spectra using the CDNN program (version 2.1), with a set of 23 reference proteins.

Thermal denaturation experiments were performed with the same samples used above. The temperature of the cell holder was increased from 5 to 90 °C at 20 °C/h rate, recording ellipticity at 222 nm. Melting temperature (T_m) values, corresponding to 50% unfolding of the protein, were obtained by non-linear curve fitting.

2.6. Intrinsic tryptophan fluorescence emission

Corrected fluorescence spectra of 5 μM solutions of Kid wild-type and mutant proteins in buffer 100 mM Na Phosphate, pH 7.0, were measured with a Fluorolog-3 spectrofluorometer system using 5×10 mm optical path length quartz cuvettes, following excitation at 282 nm. Excitation and emission bandpasses were set to 1 and 5 nm. Measurements were performed at 5 °C and all protein emission spectra were corrected by substraction of buffer blanks.

3. Results

3.1. Missense mutations in Kid that affect toxicity but not auto-regulation

We have previously reported the isolation of a collection of Kid mutants selected among cells that survived the production of Kid in the absence of a functional Kis antitoxin (Hargreaves et al., 2002b). The procedure for this selection was based on the use of pAB1120, a R1-derived plasmid that contains the mutant *parD* operon *kis74*(amber), *kid*+. In the absence of suppression of the *kis74* mutation, i.e., upon transformation of a *supF*ts strain and subsequent incubation at 42 °C, an inactive form of the Kis antitoxin is produced, thus leading to a Kid-dependent inhibition of colony formation. Therefore, to search for mutations in *kid* that disrupted the toxicity of the protein, we mutagenized the pAB1120 plasmid, used it to transform the *supF*ts strain OV2, and selected for survivors at 42 °C (Hargreaves et al., 2002b). This approach led to the isolation of a collection of single missense mutations that involved a total of 11 residues of the Kid protein (Hargreaves et al., 2002b; Fig. 1). The changes were clustered in two discrete regions bounded by residues V9 to T29 and G70 to P94 (Fig. 1).

For the 11 mutants that were selected, the loss of toxic activity of the protein seemed to be complete, at least under the conditions that were used (see above), as shown by the total recovery in viability that was observed at 42 °C (Fig. 2A). However, Kid not only interacts with a host target to inhibit cell proliferation, but also with the Kis antidote to form a complex that is required for auto-regulation of *parD* expression. Therefore, in order to evaluate the degree of specificity of the selected non-toxic mutations, it was important to test their possible effect on auto-regulation. Thus, the non-toxic pAB1120 derivatives were used to transform the MLM373 strain (*supE*, *Δlac*) containing, as a reporter of *parD* expression, a mini-F plasmid that bears the *lacZ* gene under the control of the *parD* promoter. When the wild-type *kid* gene was present (pAB1120 plasmid), the expression of the *parD* promoter dropped to 20% of the full-derepression values obtained in the absence of

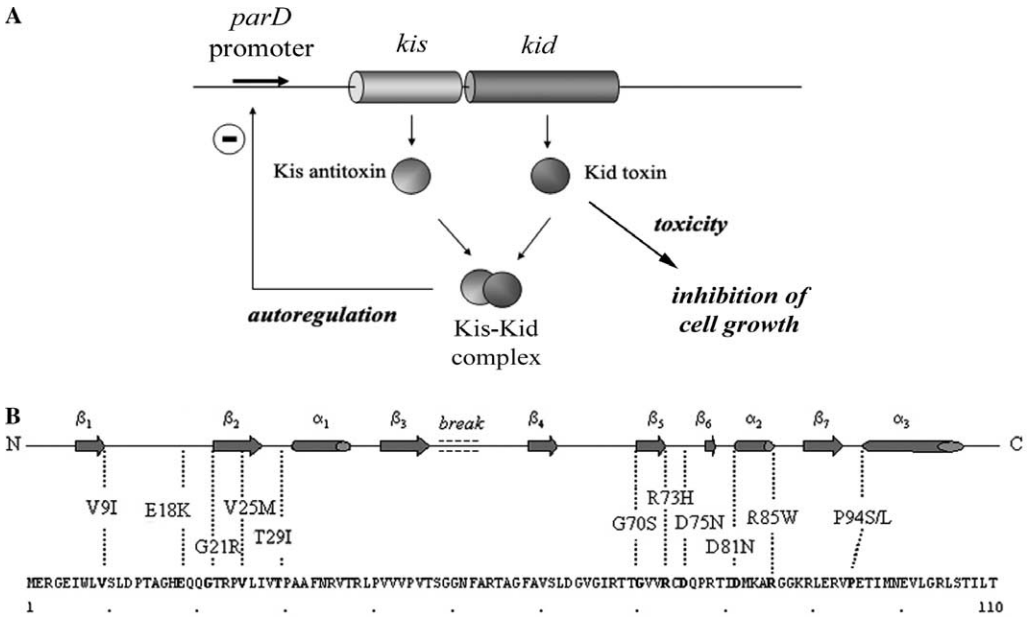

Fig. 1. (A) *parD* operon. Cilinders indicate the two genes of the operon (*kis* and *kid*), circles the Kis and Kid proteins and the arrow the *parD* promoter/operator region. The auto-repression of the operon mediated by the Kis–Kid complex is indicated by an encircled dash. (B) Localisation of the non-toxic mutations on the Kid sequence. Secondary structure elements revealed by the crystal structure of Kid (top): arrows, β-sheets; cylinders, α-helices (Hargreaves et al., 2002b). The 11 missense non-toxic mutations are shown, and residues involved are marked in bold in the Kid amino-acid sequence (bottom).

pAB1120 plasmid, as monitored by β-galactosidase activity measurements (Fig. 2B). The non-toxic mutations could be classified in two groups: (i) mutations that lead to a significant loss of auto-regulation activity, as compared to the wild-type Kid protein. This group included the Kid mutants T29I, G70S, and P94L; (ii) the rest of the mutations lead to auto-regulation levels comparable to those obtained with the wild-type Kid protein (Fig. 2B). While mutations from the former group affected both toxicity and auto-regulation, the latter group defined mutations that met our requirements for specificity, i.e., they led to loss of toxicity without interfering with the auto-regulatory activity of the Kid protein.

3.2. Mutations E18K and R85W involve residues that are conserved in related bacterial toxins

Considering that (i) Kid and ChpAK share significant similarity at the amino-acid level (26% identical and 64% conserved residues; Masuda et al., 1993); (ii) ChpAK and RelE are protein synthesis inhibitors that probably share the same mode of action (Pedersen et al., 2002); and (iii) Kid, ChpAK, and RelE are members of TA modules that are active in *E. coli* and that have similar genetic organization and auto-regulation characteristics, it seems reasonable to hypothesize that these bacterial toxins could share a common structural fold that has been conserved during evolution. Therefore, we investigated whether some of the Kid non-toxic mutations would affect conserved residues by performing a sequence alignment of Kid, ChpAK, and RelE. It appeared that residues E18 and R85, affected in the changes E18K and R85W, were the only ones to be conserved in the three toxins (Fig. 3A). Strikingly, the three-dimensional structure of Kid revealed that residues E18 and R85 interact by making a salt-bridge that contributes to link the two protomers of Kid dimer (Fig. 3B). This suggests that the E18–R85 interaction is relevant in the toxic activity of Kid protein. Moreover, it strengthens our hypothesis that Kid, ChpAK, and RelE could share structural and functional characteristics.

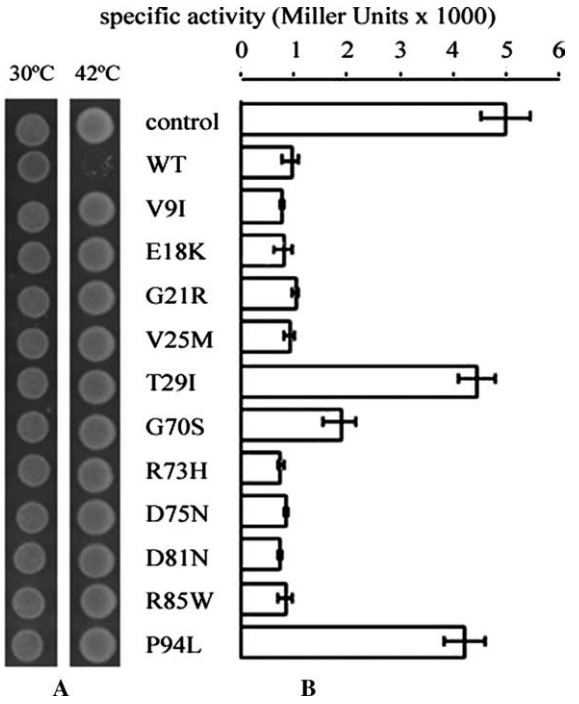

Fig. 2. Toxicity and auto-regulation assays. (A) OV2 cells containing the different mutant pAB1120 plasmids were grown to mid-exponential phase in LB broth containing kanamycin (50 μg/ml) at 30 °C. Aliquots of the cultures were spotted on two plates of the same medium solidified with agar and incubated at 30 °C (left panel) or 42 °C (right panel). Photographs were taken after a 18 h incubation. The "control" was OV2 with the pET80 plasmid that bears the wild-type *parD* operon. (B) MLM373 cells containing the pMLM132 reporter plasmid (Section 2) and the different pAB1120 plasmids were grown to mid-exponential phase in LB broth containing kanamycin (50 μg/ml) and chloramphenicol (20 μg/ml) at 37 °C. β-Galactosidase activity was measured from aliquots of the cultures as described (Miller, 1972). The "control" was the MLM373 cells containing the pMLM132 and a compatible *parD*$^-$, *kan*$^+$ replicon, pFUS2.

Therefore, we concentrated our studies in the Kid variants E18K and R85W to further investigate them at the biochemical and biophysical levels.

3.3. Biophysical characterization of KidE18K and KidR85W

The in vivo ability of Kid variants E18K and R85W to co-regulate the *parD* operon strongly suggested that these proteins interact efficiently with the antitoxins. Indeed, the Kid mutant proteins were purified using a protocol that relies initially on the formation of a His–Kis/Kid complex (Section 2). The purified proteins were further analyzed in a series of biophysical experiments, in order to determine their association state, secondary structure and the possible local structural changes induced in the protein by the mutations.

Analysis of the association state of the Kid wild-type and the two mutant proteins E18K and R85W by sedimentation equilibrium indicated that over the range of concentrations analyzed (5–45 μM), these proteins formed complexes of $M_{w,a}$ of 23,700 (± 1000), 24,700 (± 1500), and 23,600 (± 700) Da, respectively (Fig. 4). These molecular masses correspond essentially to a dimer of Kid (M_w: 23,760 Da), indicating that the mutations do not alter the quaternary structure of the protein. The sedimentation coefficient $S_{20,w}$ of wild-type Kid dimer under closely related conditions was 2.39 (± 0.05) S and its relative frictional coefficient f/f_o was 1.14, indicating a globular protein (data not shown; Section 2).

Circular dichroism spectroscopic analyses showed that the overall shape of the spectra of the two mutants and the wild-type protein were similar (Fig. 5A). Deconvolution analysis using the CDNN program indicated that, with minor differences in the content of the anti-parallel β-sheet component (31% for KidE18K, 30% for KidR85W, and 26% for Kid), the percent of secondary structure elements is similar in the three proteins. This suggests that they share a common structural fold. Analysis of the thermal stability of these mutants (Fig. 5B) showed subtle differences with respect to the wild-type protein: while E18K presented a T_m (temperature at which 50% of the protein molecules are unfolded) of 68.8 °C, close to the T_m value of the wild-type protein (70.0 °C), R85W had a T_m significantly lower (65.4 °C). This suggests that, although the mutations could locally affect the stability of Kid, no differences in the overall fold of the protein are expected to occur at physiological temperatures (30–42 °C).

The possible variations induced by non-toxic mutants in the tertiary structure of Kid were also monitored by analyzing the fluorescence emission corresponding to the single tryptophan residue of the protein (W7). Tryptophan residues are very sensitive to their local environment and thus

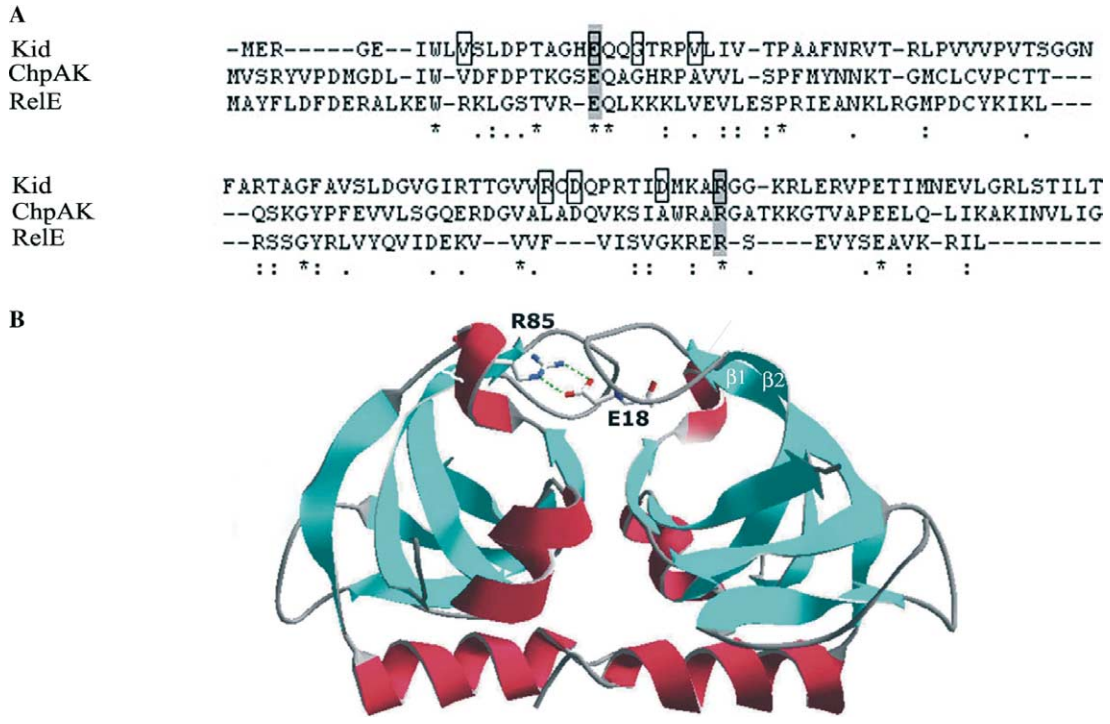

Fig. 3. (A) Sequence alignment of Kid, ChpAK, and RelE proteins. Alignments were performed with Clustal-W (www.ch.embnet.org). Opening gap penalty was set to 5. Kid residues modified by the non-toxic mutations are highlighted by empty boxes. The conserved E18 and R85 residues are shaded in gray. Dots and asterisks indicate equivalent and identical residues, respectively. (B) Localization of the E18 and R85 residues in the Kid structure. α-Helices are shown as red coils, β-strands are shown as blue arrows. R85 and E18 interact by forming a salt-bridge (dotted lines). For clarity, the R85 and E18 residues as well as the β1 and β2 strands corresponding to one of the protomers are indicated.

changes in emission spectra are frequently observed in response to factors that affect the electronic environment surrounding the indole ring. Because of the absence of tyrosine residues in Kid protein, fluorescence was excited at 282 nm, the wavelength at which maximum absorption occurred, and emission can be attributed to the single tryptophan of the protein, W7. The emission maximum was at 322 nm (Fig. 6). These properties indicate a buried tryptophan (Lakowicz, 1999). Indeed, in the crystal structure of Kid, this residue is buried in a hydrophobic core close to residue E18 affected by the E18K mutation (Hargreaves et al., 2002b). Note that mutation R85W was not analyzed because of the complexity derived from the additional tryptophan in the protein.

The emission spectrum of the KidE18K protein shifts its maximum to longer wavelengths in comparison with the spectrum of the wild-type Kid protein (Fig. 6). The slight but significant red-shifted displacement (2 nm approximately) reflects subtle changes in the local structure surrounding residue W7 in the mutated protein variants.

Altogether, these results indicate that the mutations E18K and R85W do not alter drastically the overall structure of Kid. However, the heat denaturation profiles and the fluorescence analysis suggests that the mutations could affect the conformation of structural elements at the amino-terminus of the protein.

4. Discussion

Our work shows that mutations in Kid that disrupt the cytotoxicity of the protein are located

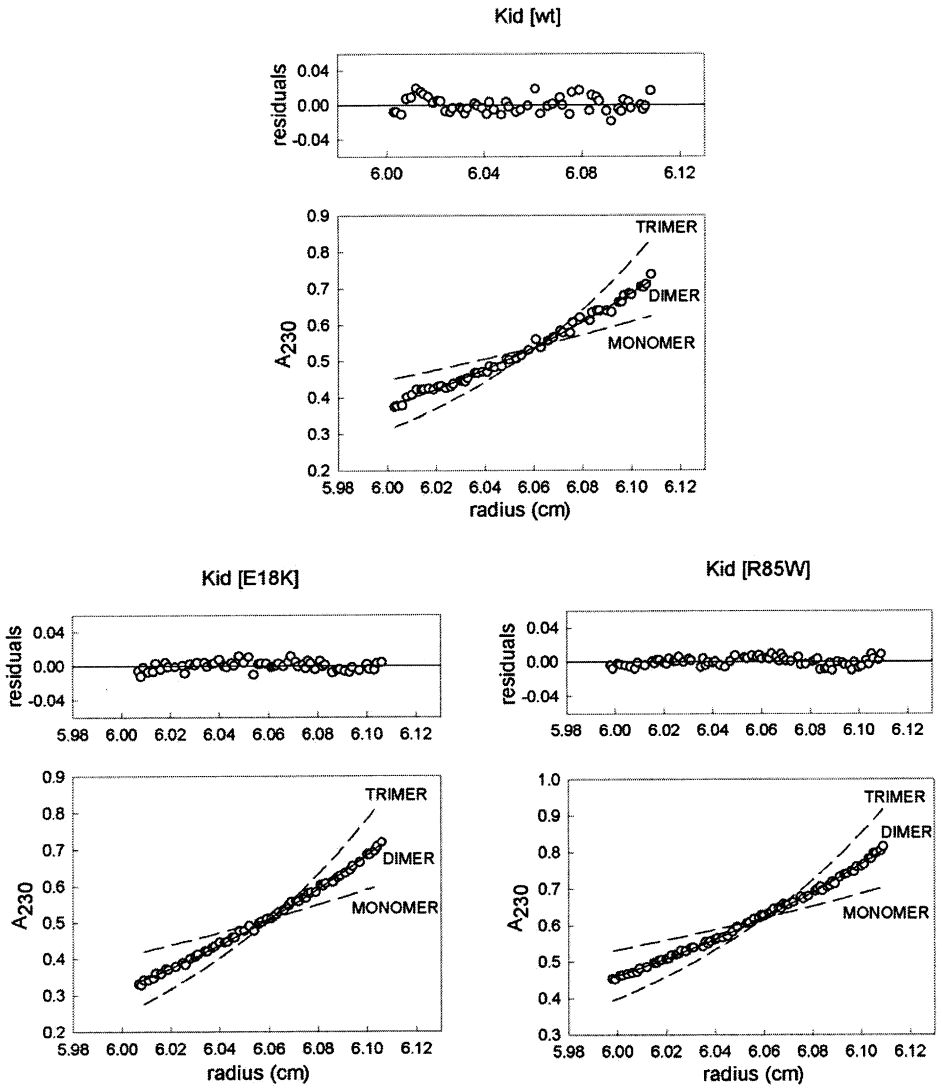

Fig. 4. Sedimentation equilibrium analysis of 30 μM Kid [wt], Kid [E18K], and Kid [R85W] proteins. Lower panels: sedimentation equilibrium gradients obtained at 19,000 rpm, 20 °C in 100 mM phosphate buffer. Solid lines represent the best fit of the experimental data to a single ideal species. In all cases, best fit gradients correspond essentially to a dimer of Kid [wt] ($M_{w,a} = 23,760$ Da, see Section 3). Dashed lines correspond to the theoretical fit to monomer ($M_{w,a} = 11,880$ Da) and trimer ($M_{w,a} = 35,640$ Da) of Kid. The residuals of the fits are shown in the upper panels.

in two discrete regions at the amino and carboxy-terminal ends. Out of 11 amino-acid changes that affected Kid toxicity, only three also affected at the same time the co-regulatory activity of the protein in vivo. The remaining eight were therefore specifically involved in toxicity. Non-toxic mutants of CcdB, the toxin of the *ccd* system from plasmid F, have been isolated and characterized (Bahassi et al., 1995). This analysis indicated that the three residues at the carboxyl end of CcdB were specifically involved in toxicity. They were proposed to form part of the region of the protein that interacts with the major dimerization interface of the subunit A of the DNA gyrase, the

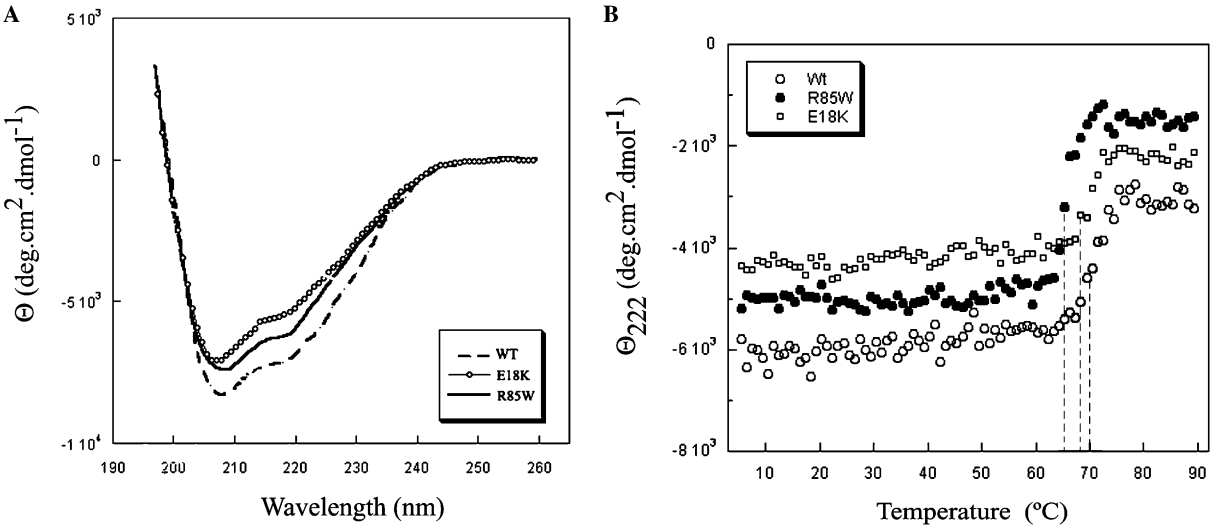

Fig. 5. Circular dichroism (A) and thermal denaturation analysis (B) of Kid wild-type and mutant proteins in 100 mM phosphate, pH 7.0. The vertical lines (dashed) indicate the T_m value corresponding to each protein.

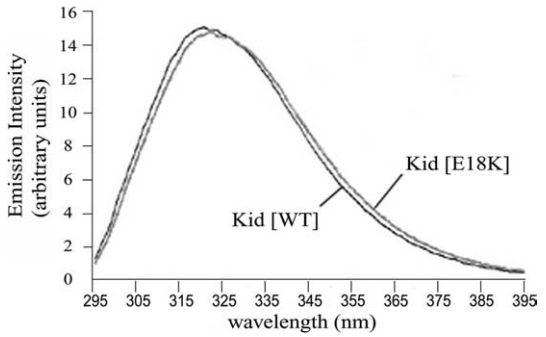

Fig. 6. Intrinsic tryptophan fluorescence emission spectra of wild-type Kid and the mutant protein Kid E18K. Protein concentrations were 5 μM in each case.

target of the CcdB toxin (Bahassi et al., 1999). In contrast, our results show that the amino-terminus of the Kid toxin plays a role in toxicity, and that a distal region in the carboxy-terminal end of the protein contributes to this function. In spite of the lack of sequence homology between Kid and CcdB, their common evolutionary origin is supported by a significant similarity in tertiary structure. However, the finding that different regions are involved in toxicity in Kid and CcdB points to the flexible character of their common structural module.

Kid mutations E18K and R85W were the only to affect residues that are conserved in the chromosomally encoded ChpAK and RelE toxins of *E. coli*. It is noteworthy that RelE mutation R81A, that abolished the toxicity of RelE (Pedersen et al., 2002), is just adjacent to the R83 residue that aligns with Kid R85. Altogether, these data suggest that the regions involved in toxicity might be conserved in these related toxins. The E18 and R85 residues are involved in a salt-bridge that links the two protomers of the Kid dimer. This interaction may be relevant in maintaining the orientation of an exposed loop located between strands β1 and β2 at the N-terminus of the protein. The recently solved structure of the ChpAK–ChpAI complex (see Note added in proof) provides additional support to this interpretation. ChpAI-mediated disruption of interactions involving R86 of ChpAK (equivalent to R85 of Kid) induces an "open" conformation in the loop between strands β1 and β2 but does not change the overall fold of the ChpAK toxin. While this suggests that this loop could could play a role in the interaction of Kid with the cellular target, defining this role will require the identification and characterization, at the structural level, of target/toxin complexes.

Neither of the amino-acid changes E18K and R85W leads to monomerization of the protein, as indicated by ultracentrifugation analysis, but the local distortion of the structure in the dimer, revealed by CD and, in the case of E18K, by fluorescence spectroscopic analyses, is sufficient for the loss of toxic activity. It is noteworthy that the detected structural change is compatible with the co-regulatory activity of the protein. This further supports that the toxicity and co-regulatory activities of the protein are basically independent functions. Definitive evidence in that sense should come from the isolation of mutants affected in auto-regulation but not in toxicity. We are currently approaching this issue.

Recent in vivo studies have shown that the *E. coli* ChpAK protein inhibits both protein synthesis and DNA replication (Pedersen et al., 2002). Moreover, the RelE toxin inhibits protein synthesis, by specifically cleaving mRNAs in the A site of the ribosome (Pedersen et al., 2003). In the case of Kid, the available indications on its mechanism of toxicity are by far less precise. Inhibition of ColE1 replication by Kid has been demonstrated both in vivo and in vitro, but to date no evidence that Kid inhibits chromosome DNA replication has been provided. Our former work has shown that overproduction of the *E. coli* replicative helicase DnaB prevented the toxic activity of Kid (Ruiz-Echevarría et al., 1995). Again, evidence supporting a direct interaction between Kid and DnaB is missing. Thus, the link between Kid and host DNA replication as a direct target of its cytotoxic activity has not been convincingly established so far. If one considers that ChpAK, a member of the Kid family of bacterial toxins, inhibits protein synthesis, and that CcdB, a toxin structurally related to Kid, is an inhibitor of DNA gyrase, then the fascinating possibility that a flexible structural module has evolved into multiple specialized proteins to reach either different or multiple targets seems a reasonable prediction. Experimental approaches to test this hypothesis rely on the future advances in the structural biology of Kid-related bacterial toxins, but also on the in vitro data to be obtained from functional studies carried out with the purified toxins.

Acknowledgments

We thank Gertrudis de Torrontegui for initial analysis of non-toxic mutants. Consolación Pardo and Ana Serrano for their excellent technical work; German Rivas for the critical reading of the manuscript; Carlos Alfonso for assistance in ultracentrifugation experiments; Kenn Gerdes and Kim Pedersen for help, support and generosity during the stay of SSS in the laboratory of KG; The Plasmid Foundation for partial financial support to S.S.-S. This research was supported by grants from the European Union (QLK2-CT-2000-00634), the Ministerio de Educación y Cultura, Spain (BIO99-0859-CO3-01), the "Programa de grupos estratégicos de la Comunidad de Madrid," 2000–2003, and the "Red Española de Investigación en Patología Infecciosa."

Note added in proof

The recent elucidation of the structure of the MazE–MazF (ChpAI–ChpAK) complex [Kamada et al., Mol. Cell 11 (2003) 875–884] confirms the relevant role in toxicity played by the loop located between strands β1 and β2. It remains to be established whether the Kid mutations discussed here, E18K and R85W, alter a conformation of this loop that is required for efficient interaction of the toxin with the cell target or whether they affect direct interactions of the E18 and R85 residues with this target.

References

Bahassi, E.M., Salmon, M.A., Van Melderen, L., Bernard, P., Couturier, M., 1995. F plasmid CcdB killer protein: *ccdB* gene mutants coding for non-cytotoxic proteins which retain their regulatory functions. Mol. Microbiol. 15, 1031–1037.

Bahassi, E.M., O'Dea, M.H., Allali, N., Messens, J., Gellert, M., Couturier, M., 1999. Interactions of CcdB with DNA gyrase. Inactivation of GyrA, poisoning of the gyrase–DNA complex, and the antidote action of CcdA. J. Biol. Chem. 274, 10936–10944.

Bernard, P., Couturier, M., 1992. Cell killing by the F plasmid CcdB protein involves poisoning of DNA–topoisomerase II complexes. J. Mol. Biol. 226, 735–745.

Bravo, A., de Torrontegui, G., Díaz, R., 1987. Identification of components of a new stability system, *parD*, of plasmid R1 that is close to its origin of replication. Mol. Gen. Genet. 210, 101–110.

Bravo, A., Ortega, S., de Torrontegui, G., Díaz, R., 1988. Killing of *Escherichia coli* cells modulated by components of the stability system *parD* of plasmid R1. Mol. Gen. Genet. 215, 146–151.

Gerdes, K., 2000. Toxin–antitoxin modules may regulate synthesis of macromolecules during nutritional stress. J. Bacteriol. 182, 561–572.

Giraldo, R., Andreu, J.M., Díaz-Orejas, R., 1998. Protein domains and conformational changes in the activation of RepA, a DNA replication initiator. EMBO J. 17, 4511–4526.

Hargreaves, D., Giraldo, R., Santos-Sierra, S., Boelens, R., Rice, D.W., Díaz-Orejas, R., Rafferty, J.B., 2002a. Crystallization and preliminary X-ray crystallographic studies on the *parD*-encoded protein Kid from *Escherichia coli* plasmid R1. Acta Crystallogr. D Biol. Crystallogr. 58, 355–358.

Hargreaves, D., Santos-Sierra, S., Giraldo, R., Sabariegos-Jareño, R., de la Cueva-Méndez, G., Boelens, R., Díaz-Orejas, R., Rafferty, J.B., 2002b. Structural and functional analysis of the Kid toxin protein from *E. coli* plasmid R1. Structure 10, 1425–1433.

Lakowicz, J.R., 1999. In: Principles of Fluorescence Spectroscopy, second ed. Kluwer Academic/Plenum Publishers, New York.

Lemonnier, M., Bouet, J.Y., Libante, V., Lane, D., 2000. Disruption of the F plasmid partition complex in vivo by partition protein SopA. Mol. Microbiol. 38, 493–505.

Loris, R., Dao-Thi, M.H., Bahassi, E.M., Van Melderen, L., Poortmans, F., Liddington, R., Couturier, M., Wyns, L., 1999. Crystal structure of CcdB, a topoisomerase poison from *E. coli*. J. Mol. Biol. 285, 1667–1677.

Masuda, Y., Miyakawa, K., Nishimura, Y., Ohtsubo, E., 1993. *chpA* and *chpB*, *Escherichia coli* chromosomal homologs of the *pem* locus responsible for stable maintenance of plasmid R100. J. Bacteriol. 175, 6850–6856.

Miller, J.H., 1972. In: Experiments in Molecular Genetics. Cold Spring Harbor Press, Cold Spring Harbor, NY, pp. 352–355.

Minton, A.P., 1994. In: Schuster, T., Laue, T. (Eds.), Modern Analytical Ultracentrifugation. Birkhauser Boston, Cambridge, MA, pp. 81–93.

Ogura, T., Hiraga, S., 1983. Mini-F plasmid genes that couple host cell division to plasmid proliferation. Proc. Natl. Acad. Sci. USA 80, 4784–4788.

Pedersen, K., Christensen, S.K., Gerdes, K., 2002. Rapid induction and reversal of a bacteriostatic condition by controlled expression of toxins and antitoxins. Mol. Microbiol. 45, 501–510.

Pedersen, K., Zavialov, A.V., Pavlov, M.Y., Elf, J., Gerdes, K., Ehrenberg, M., 2003. The bacterial toxin RelE displays codon-specific cleavage of mRNAs in the ribosomal A site. Cell 112, 131–140.

Potrykus, K., Santos, S., Lemonnier, M., Diaz-Orejas, R., Wegrzyn, G., 2002. Differential effects of Kid toxin on two modes of replication of lambdoid plasmids suggest that this toxin acts before, but not after, the assembly of the replication complex. Microbiology 148, 2489–2495.

Ruiz-Echevarría, M.J., Berzal-Herranz, A., Gerdes, K., Díaz-Orejas, R., 1991a. The *kis* and *kid* genes of *parD* maintenance system of plasmid R1 form an operon that is autoregulated at the level of transcription by the coordinate action of the Kis and Kid proteins. Mol. Microbiol. 5, 2685–2693.

Ruiz-Echevarría, M.J., de Torrontegui, G., Giménez-Gallego, G., Díaz-Orejas, R., 1991b. Structural and functional comparison between the stability systems ParD of plasmid R1 and Ccd of plasmid F. Mol. Gen. Genet. 225, 355–362.

Ruiz-Echevarría, M.J., Giménez-Gallego, G., Sabariegos-Jareño, R., Díaz-Orejas, R., 1995. Kid, a small protein of the *parD* stability system of plasmid R1, is an inhibitor of DNA replication acting at the initiation of DNA synthesis. J. Mol. Biol. 247, 568–577.

Simons, R.W., Houman, F., Kleckner, N., 1987. Improved single and multicopy lac-based cloning vectors for protein and operon fusions. Gene 53, 85–96.

Tam, J.E., Kline, B.C., 1989. The F plasmid *ccd* autorepressor is a complex of CcdA and CcdB proteins. Mol. Gen. Genet. 219, 26–32.

Tsuchimoto, S., Ohtsubo, E., 1993. Autoregulation by cooperative binding of the PemI and PemK proteins to the promoter region of the *pem* operon. Mol. Gen. Genet. 237, 81–88.

Communicated by M. Espinosa